

Research Article

Phytochemical Insights into *Rhizophora stylosa*: pH-Dependent Extraction, Antioxidant Activity, and Enzyme Inhibition Potential

Dwi Bagus Pambudi ^{1,2}  

Muhtadi ^{3*}  

Maryati ³  

¹Doctoral Program of Pharmacy, Universitas Muhammadiyah Surakarta, Surakarta, Central Java, Indonesia

²Department of Pharmacy, Universitas Muhammadiyah Pekajangan Pekalongan, Pekalongan, Central Java, Indonesia

³Department of Pharmacy, Universitas Muhammadiyah Surakarta, Surakarta, Central Java, Indonesia

*email: muhtadi@ums.ac.id; phone: +6282136362763

Keywords:

Mangrove
pH Modulation
Rhizophora stylosa
Total Flavonoid Content
Total Phenolic Content

Abstract

The solvent properties, including pH, highly influence the extraction efficiency of these bioactive compounds. This study investigated the effect of pH modulation in the ethanol solvent on the recovery of antioxidants from *Rhizophora stylosa*. Ethanolic extraction was performed on *R. stylosa* samples using solvents adjusted to varying pH levels (4, 8, 9, 10, and 12). The total phenolic content (TPC) and total flavonoid content (TFC) of the extracts were quantified using standard colorimetric assays. The antioxidant activity was evaluated using the DPPH (2,2-diphenyl-1-picrylhydrazyl) radical scavenging assay. The inhibitory activity against carbohydrate-digesting enzymes was assessed through α -amylase and α -glucosidase inhibition assays. Additionally, data mining of established natural product databases (KNAPSAcK and IMPPAT) and literature was conducted to identify and catalog the known bioactive constituents of *R. stylosa*. The results demonstrated a significant correlation between the pH of the extraction solvent and the yields of phenolic compounds, flavonoids, and the resulting antioxidant activity. Extract obtained at pH 10 yielded the highest TPC and exhibited the strongest antioxidant activity, whereas the highest TFC was observed at pH 4. Furthermore, enzymatic inhibition assays revealed that the pH 10 extract displayed moderate α -amylase inhibitory activity ($IC_{50} = 76.7 \mu\text{g/mL}$) but substantially weaker α -glucosidase inhibition ($IC_{50} = 190 \mu\text{g/mL}$), demonstrating a selective inhibition profile though less potent than that of acarbose. These findings establish pH-modulated extraction as a targeted strategy to produce potent, phenolic-rich antioxidant extracts from *R. stylosa*, highlighting its potential for nutraceutical and pharmaceutical applications.

Received: October 16th, 2025

1st Revised: January 27th, 2026

Accepted: February 3rd, 2026

Published: March 30th, 2026



© 2026 Dwi Bagus Pambudi, Muhtadi, Maryati. Published by Institute for Research and Community Services Universitas Muhammadiyah Palangkaraya. This is an Open Access article under the CC-BY-SA License (<http://creativecommons.org/licenses/by-sa/4.0/>). DOI: <https://doi.org/10.33084/bjop.v9i1.11158>

INTRODUCTION

The global quest for potent natural antioxidants has gained significant momentum, driven by the recognition that oxidative stress is a central mechanism in the pathogenesis of various chronic diseases. Notably, in diabetes, chronic hyperglycemia induces oxidative stress, which in turn contributes to insulin resistance and the progression of diabetic complications. This reality, coupled with growing concerns about the potential health risks of synthetic antioxidants, has redirected research toward the discovery of safer, natural alternatives^{1,2}. Consequently, scientific interest has shifted toward plant-derived bioactive compounds, which offer a more sustainable and biocompatible profile. Mangrove ecosystems, characterized by their unique saline and hypoxic environments, have become a focal point in this pursuit^{3,4}. Due to these environmental stressors, mangrove species synthesize a wide variety of specialized secondary metabolites with robust defense capabilities, making them an understudied yet valuable reservoir for novel therapeutic agents.

Among these resilient species, *Rhizophora stylosa* stands out as a particularly promising candidate. As a dominant mangrove species, it has a large ecological footprint and has been traditionally used in folk medicine for its purported healing properties⁵. Previous investigations suggest the presence of key bioactive compounds, including flavonoids, phenolics, and triterpenoids, in its tissues^{4,6}. However, the potential of *R. stylosa* remains largely untapped, primarily due to a lack of systematic scientific investigation aimed at optimizing the recovery of its bioactive constituents. The effectiveness of any plant-based extract is heavily dependent on the extraction procedure, where variables such as solvent pH are essential yet often overlooked in determining the solubility, stability, and ultimate bioactivity of the target molecules⁷.

The simultaneous challenges of biodiversity loss and the rising demand for natural therapies underscore the urgency of this study. Mangrove forests are among the world's most threatened ecosystems, currently facing rapid deforestation⁸. Therefore, comprehensively studying species like *R. stylosa* is not only a scientific imperative but also a conservation priority. By identifying high-value applications for its metabolites, we can establish an economic incentive for the preservation and sustainable management of these vital coastal forests. Furthermore, optimizing extraction processes maximizes yield and efficiency, thereby reducing waste and enhancing the economic viability of utilizing these natural resources⁹.

Accordingly, this study is designed to address this critical gap by systematically investigating the influence of solvent pH adjustment on the extraction efficiency of antioxidants from *R. stylosa*. The principle guiding this investigation is that pH manipulation directly affects the solubility and stability of ionizable bioactive compounds. The approach is grounded in the theory that alkaline conditions may enhance the extraction of phenolic compounds through saponification and cell wall disruption¹⁰, while specific pH levels may stabilize certain pH-sensitive flavonoids¹¹. By establishing a definitive correlation between extraction parameters and bioactivity, this research aims to provide a scientifically grounded method for harnessing the full phytochemical potential of this mangrove species, contributing to the development of standardized natural antioxidant products while highlighting the inherent value of biodiversity conservation.

MATERIALS AND METHODS

Materials

The biological material for this investigation comprised 300 g of dried leaf powder derived from *R. stylosa* specimens. These samples were strategically obtained from various coastal locations across Central Java, ensuring a diverse representation of the regional mangrove flora. To ensure taxonomic accuracy, the plant material was formally authenticated at the Faculty of Pharmacy, Universitas Muhammadiyah Surakarta, and voucher specimens were retained for reference. Analytical-grade chemical reagents were utilized for all extraction and quantification procedures. The primary solvent systems included 96% ethanol, absolute methanol, dimethyl sulfoxide, and distilled water, with pH adjustments made by precise application of 1 M HCl and 1 M NaOH.

Quantitative phytochemical analysis was performed using Folin-Ciocalteu reagent, 7.5% and 0.2 M Na₂CO₃, and 2% methanolic AlCl₃, while antioxidant capacity was assessed using 2,2-diphenyl-1-picrylhydrazyl (DPPH). For the enzymatic inhibition assays, high-purity α -amylase and α -glucosidase were used, along with their respective substrates, soluble starch (0.5%) and p-nitrophenyl- α -D-glucopyranoside (pNPG, 0.5 mM). Analytical standards, including gallic acid, quercetin, and acarbose, served as calibration standards. All biochemical reactions were stabilized using 0.01 M and 0.1 M phosphate buffers adjusted to pH 7.0, with an iodine solution (0.5%) utilized for starch-endpoint detection.

Methods

Extraction of Rhizophora stylosa with pH adjustment

A total of 300 g of dried *R. stylosa* leaf powder was partitioned into equal subsets to evaluate extraction efficiency under varied pH conditions. Each batch underwent exhaustive maceration with 96% ethanol, with the solvent pH pre-adjusted to 4, 8, 9, 10, and 12 by the meticulous dropwise addition of 1 M HCl or 1 M NaOH. This extraction process was repeated for five consecutive 24-hour cycles for each pH variant, complemented by two additional remaceration steps to ensure maximum compound recovery. The resulting filtrates for each pH level were isolated and concentrated under reduced pressure at 50°C. To safeguard the integrity of thermolabile bioactive molecules, all final yields were further concentrated at 40°C before being secured in amber vials for subsequent downstream analyses^{12,13}.

Phytochemical composition

The TPC was quantified through the Folin-Ciocalteu colorimetric method. In this procedure, 0.5 mL of methanolic extract (1 mg/mL) was reacted with 2.5 mL of 10% Folin-Ciocalteu reagent for 5 minutes, then alkalized with 2 mL of 7.5% Na₂CO₃. After a 30-minute incubation at 40°C in the dark, absorbance was measured at 765 nm. Phenolic concentrations were interpolated from a gallic acid standard curve (0–100 µg/mL) and reported as mg gallic acid equivalents per gram of dry extract (mg GAE/g)^{14,15}. Similarly, the TFC was appraised using AlCl₃ assay, where 1 mL of extract was combined with 2% methanolic AlCl₃. After a 30-minute ambient incubation, the absorbance of the flavonoid-aluminum complex was measured at 415 nm. Results were calculated against a quercetin calibration curve (0–100 µg/mL) and expressed as mg quercetin equivalents per gram of extract (mg QE/g)¹⁶.

DPPH radical scavenging activity assay

The *in vitro* antioxidant capacity of the extracts was determined using the DPPH free radical scavenging assay, modified for high-throughput analysis¹⁷. A 0.2 mM stock solution of DPPH was freshly prepared in absolute methanol and protected from light. Test samples were serially diluted in methanol to achieve a concentration gradient of 1 to 10 mg/mL. The assay was conducted in 96-well microplates, where 100 µL of each sample concentration was combined with 100 µL of the DPPH solution, homogenized, and incubated in the dark for 30 minutes. Negative controls utilized methanol in place of the sample, while blanks were corrected for inherent sample pigmentation. Absorbance was measured at 520 nm, and the percentage of inhibition was calculated using **Equation 1**. Antioxidant potency was quantified as the half-maximal inhibitory concentration (IC₅₀), determined from a linear regression of the concentration-inhibition plot. All experimental runs were performed in triplicate to ensure statistical reliability.

$$\% \text{inhibition} = \frac{\text{Control absorbance} - \text{Sample absorbance}}{\text{Control absorbance}} \times 100\% \quad [1]$$

Spectroscopic characterization

Electronic transitions in *R. stylosa* extracts were investigated by UV-Vis spectroscopy using a Shimadzu UV-1280 spectrophotometer. Each extract was diluted with its corresponding pH-adjusted ethanol solvent to maintain chemical consistency during analysis across a wavelength range of 200 to 800 nm¹⁸. Furthermore, FTIR spectroscopy was employed to map the functional groups using a Shimadzu IRSpirit spectrometer equipped with a QATR™-S Single Reflection ATR accessory. Spectra were recorded from 4000 to 500 cm⁻¹ at a resolution of 4 cm⁻¹, with 45 scans accumulated per sample to maximize the signal-to-noise ratio and ensure high-fidelity structural identification¹⁹.

Assessment of α-amylase and α-glucosidase inhibitory activity

The evaluation of α-amylase inhibition followed a systematic multi-step protocol, beginning with the preparation of a 0.01 M phosphate buffer at pH 7.0. Test samples and fractions were dissolved in DMSO and diluted to a primary concentration of 1000 µg/mL; further working dilutions were prepared at concentrations between 25 and 100 µg/mL. An enzymatic solution of α-amylase (0.5128 U/mL) was reacted with a 0.5% starch substrate, using acarbose as a reference inhibitor. Following sequential 10-minute and 15-minute incubations at 37°C, the reaction was terminated with a 0.5% iodine solution, and absorbance was recorded at 540 nm²⁰. In parallel, α-glucosidase inhibition was assessed by assembling reaction mixtures of phosphate buffer, pNPG substrate (0.5 mM), test samples (500 µg/mL), and enzyme solution (0.04 U/mL). After a 30-minute incubation at 37°C, the reaction was halted with 0.2 M Na₂CO₃, which also intensified the yellow coloration of the liberated p-nitrophenol. Quantitative analysis was performed at 410 nm, with all determinations conducted in triplicate²¹.

Data-driven phytochemical profiling of *Rhizophora* species

A comprehensive chemical census of *R. stylosa* was established through an integrative computational-bibliographic framework. This strategy used major natural product repositories, including the KNApSACk Family database to retrieve documented secondary metabolites²² and the IMPPAT database to cross-reference phytochemical profiles with their known biological activities²³. This digital exploration was synthesized with a rigorous examination of the existing scientific literature

to ensure exhaustive coverage. Strategic search queries, including "*Rhizophora stylosa* chemical compounds," were systematically applied across multiple digital platforms to compile a definitive phytochemical inventory for the species.

Data analysis

Quantitative data were analyzed using the R statistical computing environment (version 2025.05.1). The analytical workflow was categorized based on the underlying data distribution, which was initially evaluated for normality via the Shapiro-Wilk test. For datasets meeting the normality criteria, the homogeneity of variances was confirmed using Levene's test. Data conforming to these parametric assumptions were subjected to a one-way ANOVA. When significant differences were detected, post hoc comparisons were conducted using Tukey's HSD test. All statistical evaluations were conducted at the $\alpha = 0.05$ significance threshold to ensure the rigor of the findings.

RESULTS AND DISCUSSION

Statistical analysis revealed that extraction pH had a highly significant effect on total phenolic content ($F(4,10) = 41.51$, $p < 0.0001$). Post-hoc Tukey HSD analysis identified specific differences, most notably that extraction at pH 8 resulted in a significantly lower phenolic yield (36.56 ± 2.97 mg GAE/g) than in all other cohorts ($p < 0.0001$ for pH 4, 9, and 10; $p < 0.001$ for pH 12). Conversely, the highest yields were recorded at pH 10 (91.16 ± 5.50 mg GAE/g) and pH 4 (86.69 ± 2.80 mg GAE/g), which were statistically indistinguishable. In parallel, the extraction pH significantly influenced flavonoid content ($F(4,10) = 10.55$, $p = 0.0013$), with a peak at pH 4 (10.41 ± 0.38 mg QE/g). A significant reduction was observed at pH 12 (5.57 ± 1.07 mg QE/g) and pH 10 (5.74 ± 0.19 mg QE/g), suggesting that specific flavonoid classes may undergo degradation in highly basic environments. These relationships are detailed in **Figure 1**.

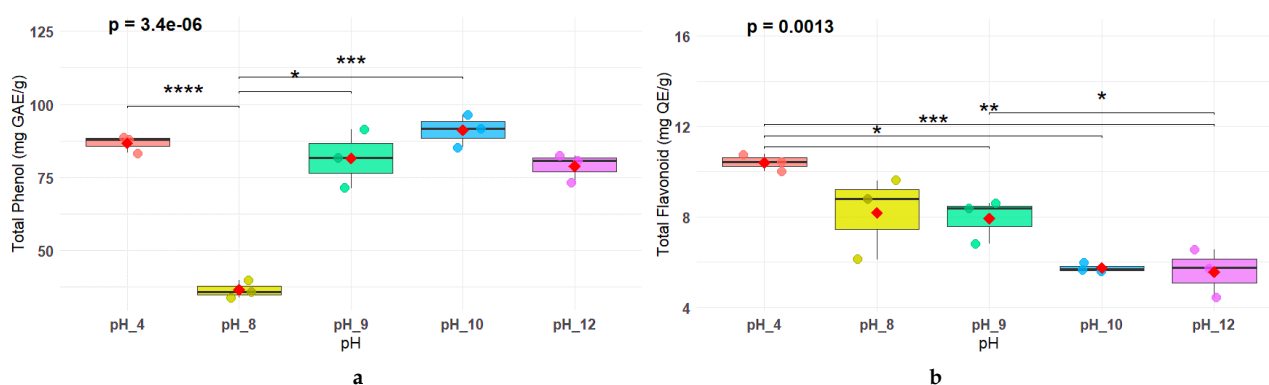


Figure 1. The effect of extraction pH on the (a) TPC and (b) TFC of *R. stylosa* extract. Data are presented as mean \pm SD ($n=3$). Statistical significance between groups was determined using a one-way ANOVA followed by Tukey's post hoc test. Asterisks (*) indicate significant differences compared to the pH 4 group: * $p < 0.05$, ** $p < 0.01$, *** $p < 0.001$, ns indicates no significant differences.

The significant variation in TPC and TFC content across the pH spectrum underscores the critical role of solvent alkalinity in modulating the solubility and stability of *R. stylosa* metabolites. The peak phenolic yield at pH 10 is likely facilitated by the alkaline-induced hydrolysis of ester and ether bonds that tether phenolic acids to the lignocellulosic matrix of the plant cell wall^{24,25}. This process increases the accessibility of glycosylated phenolics, which often remain sequestered in acidic or neutral media. Conversely, the drastic reduction in TFC at pH 12 suggests that while alkalinity aids extraction, extreme basicity triggers the ring-opening of the flavonoid C-ring or promotes the degradation of anthocyanins and chalcones. This alignment with findings in other mangrove species confirms that specific flavonoid classes possess a narrow window of stability, typically favoring near-neutral to moderately alkaline ranges²⁶.

The IC_{50} values for *R. stylosa* met all statistical assumptions for parametric analysis, including normality and homogeneity of variances (Levene's test, $p = 0.641$). A one-way ANOVA demonstrated that extraction pH significantly affected antioxidant activity ($F(4,10) = 86.44$, $p < 0.0001$). Post-hoc Tukey's HSD tests revealed that extractions at pH 8, 9, and 10 produced extracts with significantly enhanced antioxidant potency (lower IC_{50}) relative to the acidic pH 4 extract ($p < 0.001$ for all), as seen in **Figure 2a**. The highest antioxidant potency was observed at pH 10 (50.15 ± 0.38 $\mu\text{g/mL}$) and pH 8 (51.15

$\pm 3.71 \mu\text{g/mL}$), which were statistically indistinguishable. Conversely, extraction at pH 12 ($81.84 \pm 3.29 \mu\text{g/mL}$) yielded an extract with significantly weaker activity than other alkaline levels (8, 9, 10) ($p < 0.01$), though it remained more potent than the pH 4 extract ($99.83 \pm 6.06 \mu\text{g/mL}$, $p = 0.0019$). The pH 9 extract ($60.31 \pm 3.81 \mu\text{g/mL}$) demonstrated moderate potency. As anticipated, the positive control (Vitamin C) exhibited vastly superior antioxidant activity ($\text{IC}_{50} = 4.47 \pm 0.40 \mu\text{g/mL}$) compared to all plant-derived extracts (Figure 2b).

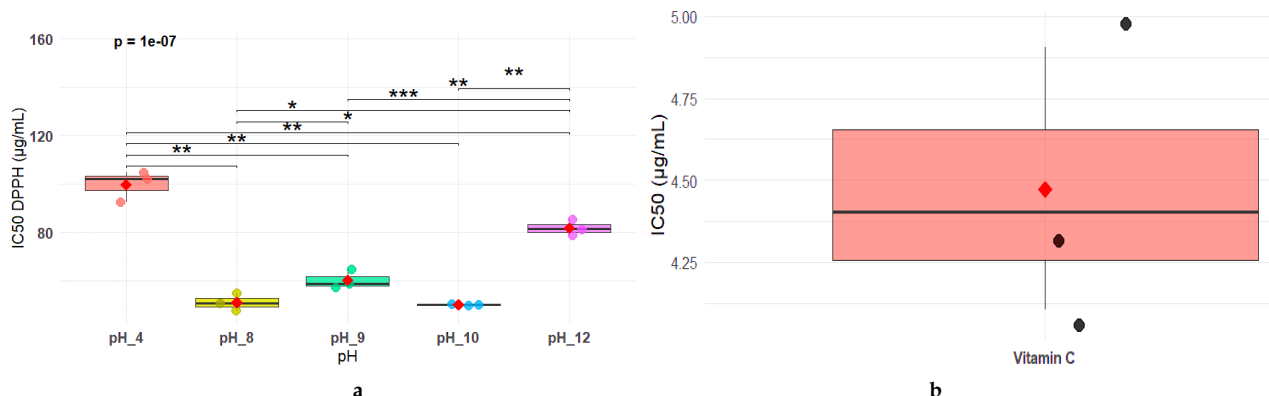


Figure 2. The effect of extraction pH on the antioxidant activity. (a) IC₅₀ values of of *R. stylosa* extract from different pH conditions. A lower IC₅₀ value indicates stronger antioxidant activity. (b) IC₅₀ value of the positive control (Vitamin C) for activity comparison. Data are presented as mean \pm SD (n=3). Statistical significance between groups was determined using a one-way ANOVA followed by Tukey's post hoc test. Asterisks (*) indicate significant differences compared to the pH 4 group: *p < 0.05, **p < 0.01, ***p < 0.001, ns indicates no significant differences.

The strong inverse correlation between IC₅₀ values and phytochemical yield²⁷ provides statistical confirmation that the antioxidant power of *R. stylosa* is predominantly driven by its phenolic constituents. However, the robust activity of the pH 10 extract, despite its significantly lower flavonoid count compared to the pH 4 group, indicates that antioxidant potency is not merely a function of total concentration. Instead, the alkaline environment at pH 10 appears to selectively recover specific phenolic subclasses, likely high-value antioxidant polymers, with exceptionally high radical-scavenging capacities²⁸. This qualitative shift in the phytochemical profile suggests that targeted pH modification can yield extracts more efficacious than those obtained by traditional bulk extraction methods.

The comparative analysis illustrated in Figure 3a reveals a discernible relationship between pH modification and the recovery of bioactive compounds. An inverse relationship was observed between phenolic recovery and IC₅₀ values, indicating that extracts with higher phenolic concentrations exhibited significantly greater radical scavenging activity. The heatmap in Figure 3b further identifies pH 10 as the optimal condition, balancing the highest total phenolic content (91.16 mg GAE/g) with peak antioxidant activity (IC₅₀ = 50.15 µg/mL). In contrast, pH 8 yielded the lowest phenolic content (36.56 mgGAE/g).

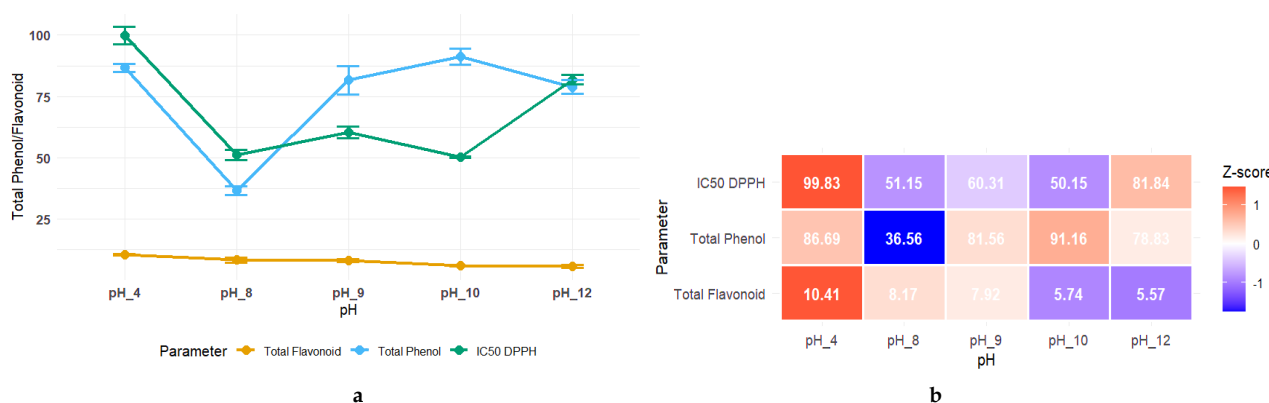


Figure 3. Multivariate analysis of the effect of extraction pH on bioactive compound yield and antioxidant activity. (a) Comparative line chart of mean total phenolic content, total flavonoid content, and IC₅₀ of *R. stylosa* across different pH conditions. (b) Heatmap of Z-score standardized values for each parameter. The color gradient represents relative performance, enabling direct visual comparison with the optimal extraction condition (pH 10).

To visualize the complex interrelationship between the measured variables, a three-dimensional scatter plot was constructed (Figure 4). The plot highlights a robust inverse correlation between IC_{50} (z-axis) and total phenolic content (y-axis), with samples with the highest phenolic concentrations consistently located within the region of maximum antioxidant potency. Although the relationship with total flavonoid content was less pronounced, the distinct clustering of data points confirms that extraction pH is a primary determinant of the extract's functional profile. Specifically, the pH 10 cohort forms a unique cluster, visually and statistically confirming its optimal status for high phenolic yield and radical scavenging. In contrast, the pH 8 extract is isolated, reflecting its status as a high-potency but low-yield variant^{29,30}.

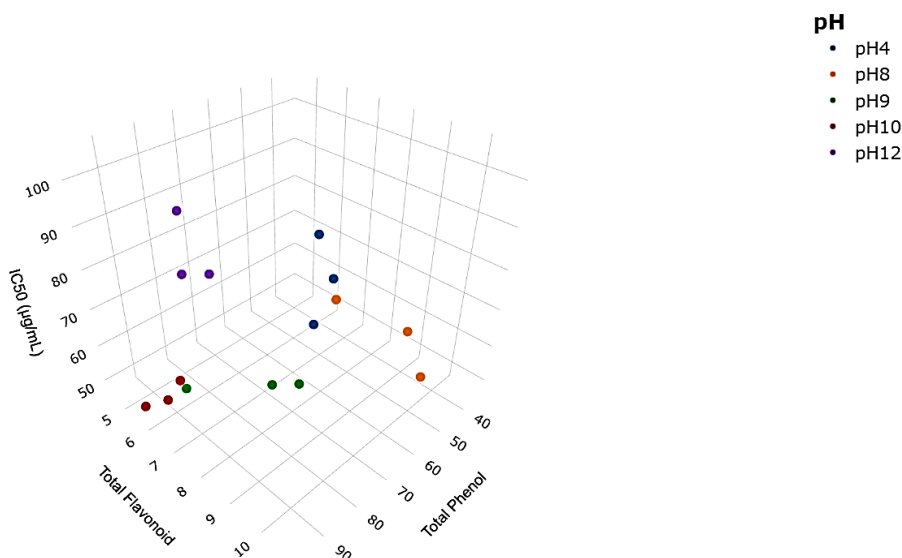


Figure 4. Three-dimensional scatter plot illustrating the relationship between antioxidant activity (IC_{50} DPPH, z-axis), TPC (y-axis), and TFC (x-axis) for extracts from different pH conditions. The clustering of data points demonstrates the dominant positive correlation between phenolic content and enhanced antioxidant power.

Remarkably, despite shifting from acidic to strongly alkaline conditions, the UV-Vis spectra (Figure 5a) remained stable, with no significant bathochromic or hypsochromic shifts. The preservation of nearly identical peak shapes in the 250–450 nm region (Figure 5b) suggests that the core chromophore systems, responsible for the primary $\pi \rightarrow \pi^*$ and $n \rightarrow \pi^*$ electronic transitions, remain structurally intact and unaffected by pH-mediated ionization^{31,32}. However, hierarchical cluster analysis (HCA) of the FTIR data (Figure 5c) provided a more nuanced perspective, segregating pH 8, 9, and 10 into a distinct group separate from pH 4 and 12. This clustering aligns with the bioactivity data, implying that moderately alkaline conditions preserve a favorable phytochemical fingerprint optimal for radical scavenging³³. The anomaly at pH 8, characterized by low yield but high activity, may relate to an isoelectric point or the formation of insoluble complexes that induce co-precipitation, demonstrating the non-linear impact of pH on plant matrices^{34,35}.

The pH 10 extract was further evaluated for its ability to modulate carbohydrate digestion. In enzymatic assays, the extract (RS- α Amy) demonstrated moderate α -amylase inhibition ($IC_{50} = 76.7 \pm 6.44 \mu\text{g/mL}$), though it was less potent than the acarbose standard (Acb-AMS, $26.9 \pm 3.64 \mu\text{g/mL}$). Its efficacy against α -glucosidase (RS- β Gls, $190 \pm 25.1 \mu\text{g/mL}$) was significantly weaker than the reference control (Acb-BGL, $0.212 \pm 0.0194 \mu\text{g/mL}$), as seen in Figure 6. These findings suggest that the extract's complex mixture may involve non-competitive interactions, whereas acarbose acts as a high-affinity oligosaccharide mimic^{36,37}.

Building upon the promising antioxidant profile of the pH 10 extract, its evaluation against carbohydrate-hydrolyzing enzymes represents a critical step in assessing its utility for managing postprandial hyperglycaemia. The observation that the extract (RS- α Amy) demonstrated moderate α -amylase inhibition while being substantially weaker against α -glucosidase is a therapeutically significant differential. Ideal anti-hyperglycaemic agents should preferentially inhibit α -glucosidase to prevent rapid glucose absorption in the small intestine while minimizing excessive fermentation of undigested starch in the colon³⁸. Such a profile helps reduce the gastrointestinal side effects, such as flatulence and diarrhea, typically associated with potent α -amylase inhibitors like acarbose.

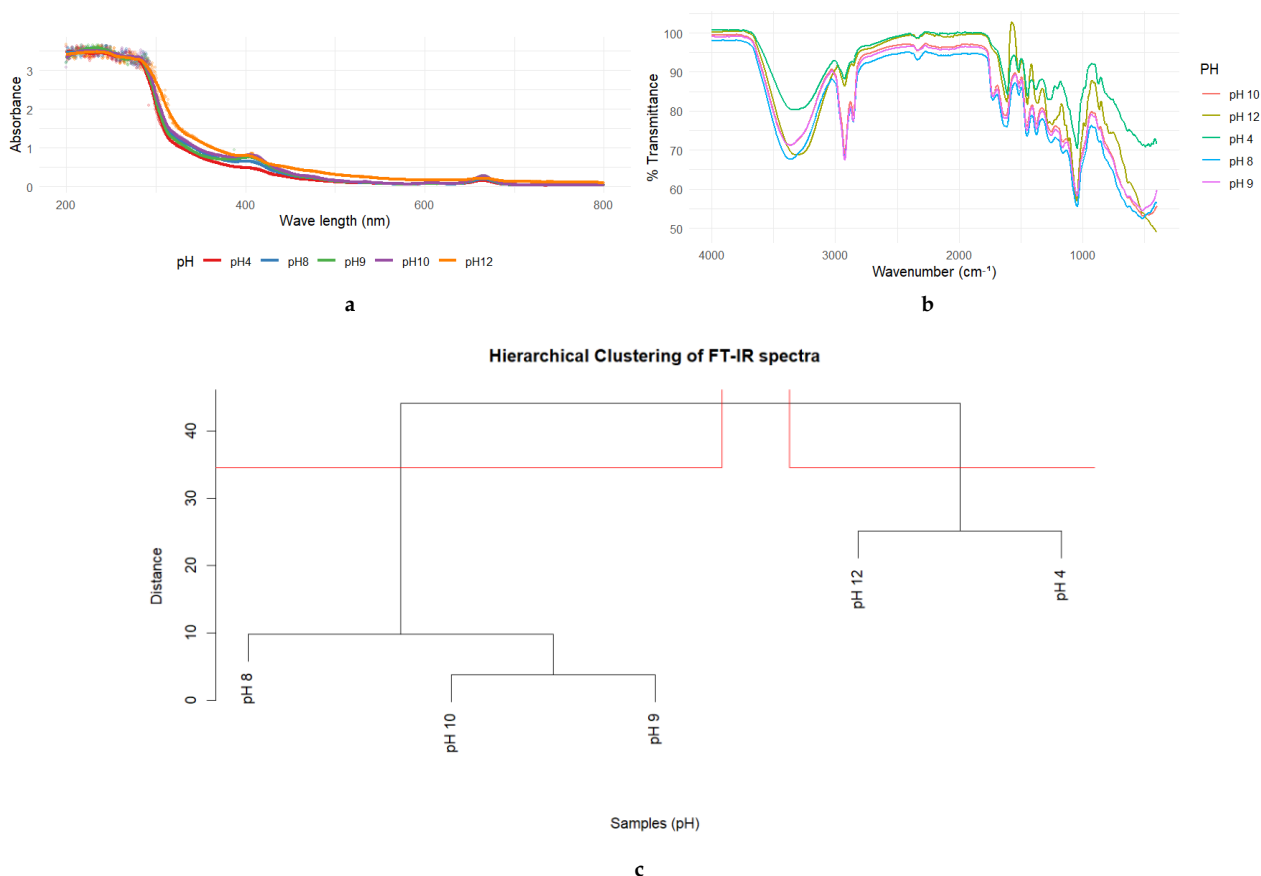


Figure 5. (a) Comparative UV-Vis spectral profiles of *R. stylosa* extracts. (b) FTIR spectroscopy analysis overlay of extracts. (c) Dendrogram resulting from HCA of FTIR data, revealing two main clusters (pH 8, 9, 10 vs. pH 4, 12).

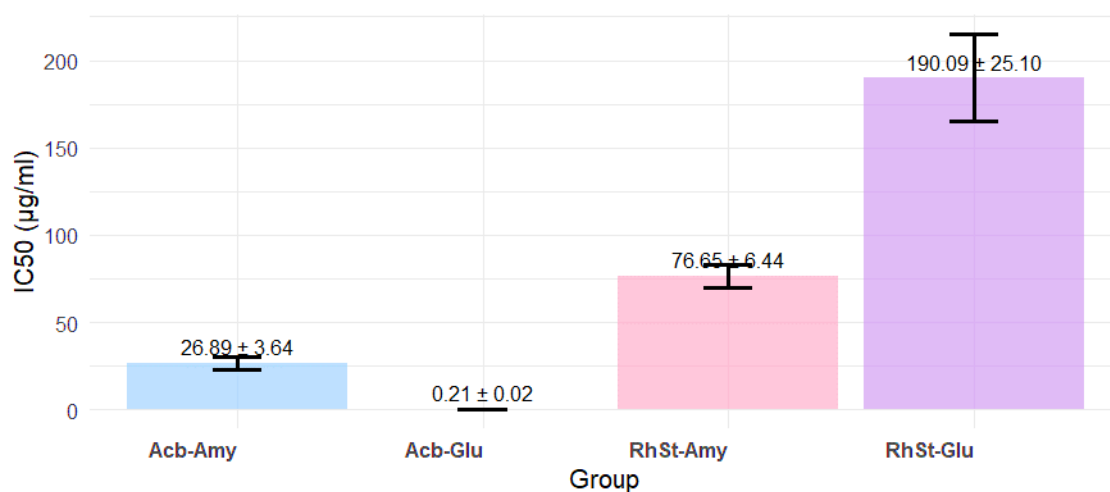


Figure 6. Enzyme inhibition potency of acarbose and *R. stylosa* extract. Lower IC₅₀ values indicate stronger inhibition. Acarbose demonstrated superior inhibition, particularly against α-glucosidase (Acb-BGL).

To explain this performance, a computational-bibliographic strategy identified a profile of 48 secondary metabolites in *R. stylosa* (Table I), characterized by a high prevalence of flavan-3-ols, such as catechins and proanthocyanidins³⁹⁻⁴². The identification of specific compounds such as taraxerol, taraxerone, careaborin, and rhizostyloide underscores the species' chemodiversity. The alkaline extraction at pH 10 likely recovers high-value polymers such as cinchonains, which possess antioxidant capacities exceeding those of simple monomers⁴³, thereby justifying the extract's robust bioactivity despite a lower flavonoid content.

Table I. Bioactive compounds identified in *R. stylosa* through data mining.

No.	Compound Name	MW (g/mol)	References
1	(-)-Epicatechin	290.27	42
2	(+)-Afzelechin	274.27	42
3	(+)-Catechin	290.27	42
4	(+)-Catechin 3-O- α -L-rhamnoside	436.40	41
5	(+)-Isolariciresinol	360.40	39
6	(+)-Pinoresinol	358.40	39
7	(6S,7E,9R)-6,9-dihydroxy-4,7-megastigmadien-3-one 9-O-[α -L-arabinopyranosyl-(1 \rightarrow 6)- β -D-glucopyranoside]	520.25	39
8	(7S,8R)-3,3',5-trimethoxy-4',7-epoxy-8,5'-neolignan-4,9,9'-triol	390.17	39
9	(7S,8R)-3,3'-dimethoxy-4',7-epoxy-8,5'-neolignan-4,9,9'-triol	360.16	39
10	(S)-2,3-Epoxy-squalene (2,3-oxidosqualene)	426.70	31
11	1,2-dimethoxybenzene	138.16	31
12	15 α -hydroxy- β -amyrin	442.38	31
13	2,3-butanediol	90.12	31
14	3,3',4',5,7-O-pentaacetyl(-)-epicatechin	500.13	31
15	3,7-O-diacetyl (-)-epicatechin	372.12	31
16	3-O-acetyl (-)-epicatechin	332.09	31
17	3 β -O-(E)-coumaroyl-15 α -hydroxy- β -amyrin	588.42	31
18	3 β -O-(Z) coumaroyl-taraxerol	574.44	31
19	3 β -taraxerol acetate	468.40	31
20	3 β -taraxerol formate	456.40	31
21	Astilbin	450.40	40
22	Blumenol A	224.14	39
23	Careaborin	572.87	42, 40
24	Cinchonain Ia	452.40	41
25	Cinchonain Ib	452.40	41
26	Cinchonain IIa	740.70	41
27	Cinchonain IIb	740.70	41
28	Cycloartenol	426.70	41
29	Eugenol	164.20	39
30	Glabaroside A	598.17	41
31	Glabaroside B	598.17	41
32	Isovanillic acid	168.15	39
33	Kaempferol 3-rutinoside	594.50	39
34	Lauric Acid	200.32	41
35	Linalool	154.25	39
36	N,N-dimethyl-L-alanine	117.15	39
37	Polystachyol	420.18	39
38	Proanthocyanidin B2	578.50	42
39	Procyanidin	594.53	5
40	Prodelfinidin	594.14	5
41	Protocatechuic acid	154.12	39
42	Quercetin-3-O-galactopyranoside	464.10	5
43	Rhizostyloide	632.43	39
44	Rutin	610.50	40
45	Taraxerol	426.73	42, 40
46	Taraxerone	424.70	40
47	β -Daucosterol	576.80	40
48	β -Sitosterol	414.70	40

The data-mined phytochemical profile including classic mangrove triterpenoids such as taraxerol and taraxerone, aligns with the chemical fingerprint expected for the *Rhizophoraceae* family⁴². The prominence of flavan-3-ols and their polymers (e.g., procyanidin B2) as the likely key antioxidants is a pivotal finding. By directly linking optimized pH extraction to peak efficacy, this study provides a targeted strategy for developing standardized *R. stylosa* extracts. Future applications should focus on isolating these specific high-value polymers to produce more potent and predictable therapeutic agents than general plant extracts.

CONCLUSION

This study demonstrates that modulating solvent pH is an effective strategy for optimizing the antioxidant potential of *R. stylosa* extracts. The alkaline pH 10 was identified as the optimal condition, yielding high phenolic content and exceptional radical scavenging activity without compromising the structural integrity of the core chromophore systems. The strong

correlation between phytochemical profiles and bioactivity, visualized through 3D multivariate mapping and confirmed by HCA clustering, underscores the critical role of targeted extraction. While the extract exhibits moderate α -amylase inhibition, its primary value lies in its potent antioxidant capacity, likely driven by the recovery of specialized flavan-3-ols and cinchonans. These results provide a robust scientific foundation for utilizing *R. stylosa* as a standardized source of high-potency antioxidants in the pharmaceutical and nutraceutical sectors. Future work should isolate specific high-activity constituents at pH 10 and evaluate their performance in complex biological systems.

ACKNOWLEDGMENT

The author extends sincere gratitude to the Research and Innovation Institute, Universitas Muhammadiyah Surakarta for awarding the Doctoral Dissertation Research grant, which provided the essential funding that made this study possible. Deep appreciation is also conveyed to Universitas Muhammadiyah Surakarta for the comprehensive institutional support, laboratory resources, and collaborative environment provided throughout the duration of this research. The contribution of these resources was fundamental to the successful execution of the experimental and analytical phases of the project.

AUTHORS' CONTRIBUTION

Conceptualization: Dwi Bagus Pambudi, Muhtadi

Data curation: Dwi Bagus Pambudi

Formal analysis: Dwi Bagus Pambudi, Muhtadi, Maryati

Funding acquisition: Muhtadi

Investigation: Dwi Bagus Pambudi

Methodology: Muhtadi, Maryati

Project administration: Dwi Bagus Pambudi

Resources: Muhtadi

Software: Muhtadi

Supervision: Muhtadi, Maryati

Validation: Muhtadi, Maryati

Visualization: Dwi Bagus Pambudi

Writing - original draft: Dwi Bagus Pambudi

Writing - review & editing: Muhtadi, Maryati

DATA AVAILABILITY

None.

CONFLICT OF INTEREST

The authors declared no conflict of interest related to this research.

REFERENCES

1. Viana MDM, Santos SS, Cruz ABO, de Jesus MVAC, Lauria PSS, Lins MP, et al. Probiotics as Antioxidant Strategy for Managing Diabetes Mellitus and Its Complications. *Antioxidants*. 2025;14(7):767. DOI: [10.3390/antiox14070767](https://doi.org/10.3390/antiox14070767). PMID: [40722870](https://pubmed.ncbi.nlm.nih.gov/40722870/); PMCID: [PMC12291856](https://pubmed.ncbi.nlm.nih.gov/PMC12291856/).
2. Wahyuni S, Mahmuda INN, Maryati, Perdana AP, Maharotullaili NA. Studi Komparatif Invitro Aktivitas Antioksidan Ekstrak Etanol, Fraksi Etil Asetat Dan Isolat Aktif Kulit Delima (*Punica Granatum L.*). *Biomedika*. 2023;15(1):67-75. DOI: [10.23917/biomedika.v15i1.1751](https://doi.org/10.23917/biomedika.v15i1.1751).

3. Lin W, Li G, Xu J. Bio-Active Products from Mangrove Ecosystems. *Mar Drugs*. 2023;21(4):239. DOI: [10.3390/md21040239](https://doi.org/10.3390/md21040239). PMID: 37103378; PMCID: [PMC10145032](https://pubmed.ncbi.nlm.nih.gov/PMC10145032/).
4. Muhtadi M, Pambudi DB, Maryati M. Mechanistic Insight into Medicinal Properties of Indonesian Diverse Mangrove Species: A Review. *Int J Appl Pharm*. 2024;16(5):1-8. DOI: [10.22159/ijap.2024v16s5.52488](https://doi.org/10.22159/ijap.2024v16s5.52488).
5. Miranti DI, Ichiura H, Ohtani Y. The Bioactive Compounds and Antioxidant Activity of Food Products of *Rhizophora stylosa* Fruit (Coffee and Tea Mangrove). *Int J For Res*. 2018;2018(1):2315329. DOI: [10.1155/2018/2315329](https://doi.org/10.1155/2018/2315329).
6. Wang Y, Zhu H, Tam NFY. Polyphenols, tannins and antioxidant activities of eight true mangrove plant species in South China. *Plant Soil*. 2014;374(1-2):549-63. DOI: [10.1007/s11104-013-1912-9](https://doi.org/10.1007/s11104-013-1912-9).
7. Ahmed S, Alsharif KF, Aschner M, Alzahrani KJ, Akkol EK, Türkançoğlu EG, et al. A deep dive into herbal extraction: Techniques, trends, and technological advancements. *S Afr J Bot*. 2026;188:9-37. DOI: [10.1016/j.sajb.2025.11.005](https://doi.org/10.1016/j.sajb.2025.11.005). PMID: 41716686; PMCID: [PMC12916026](https://pubmed.ncbi.nlm.nih.gov/PMC12916026/).
8. Heck N, Goldberg L, Andradi-Brown DA, Campbell A, Narayan S, Ahmadiya GN, et al. Global drivers of mangrove loss in protected areas. *Conserv Biol*. 2024;38(6):e14293. DOI: [10.1111/cobi.14293](https://doi.org/10.1111/cobi.14293). PMID: 38766900; PMCID: [PMC11589005](https://pubmed.ncbi.nlm.nih.gov/PMC11589005/).
9. Rajković KM, Vasić M, Drobac M, Mutić J, Jeremić S, Simić V, et al. Optimization of extraction yield and chemical characterization of optimal extract from *Juglans nigra* L. leaves. *Chem Eng Res Des* 2020;157:25-33. DOI: [10.1016/j.cherd.2020.03.002](https://doi.org/10.1016/j.cherd.2020.03.002).
10. Cabrera MN, Rossi A, Guarino JI, Felissia FE, Area MC. Alkaline Extraction and Ethanol Precipitation of High-Molecular-Weight Xylan Compounds from Eucalyptus Residues. *Polymers*. 2025;17(12):1589. DOI: [10.3390/polym17121589](https://doi.org/10.3390/polym17121589). PMID: 40574117; PMCID: [PMC12196941](https://pubmed.ncbi.nlm.nih.gov/PMC12196941/).
11. Csuti A, Zheng B, Zhou H. Post pH-driven encapsulation of polyphenols in next-generation foods: principles, formation and applications. *Crit Rev Food Sci Nutr*. 2024;64(33):12892-906. DOI: [10.1080/10408398.2023.2258214](https://doi.org/10.1080/10408398.2023.2258214). PMID: 37722872.
12. Yulyana A, Chaidir C, Simanjuntak P, Sulastri L, Abdillah S. The water fraction of Cantigi (*Vaccinium varingaefolium* Bl. Miq.) fruits demonstrate the highest antimetabolic syndrome properties on enzyme assay. *Pharmacia*. 2023;70(3):587-94. DOI: [10.3897/pharmacia.70.e109333](https://doi.org/10.3897/pharmacia.70.e109333).
13. Fajriyah NN, Muhtadi M, Rosyidand FN, Mugiyanto E. Characterization of nano-hydrogel chitosan-annona muricata extract by using ionic gelation. *AIP Conf Proc*. 2024;3070:020008. DOI: [10.1063/5.0198874](https://doi.org/10.1063/5.0198874).
14. Pérez M, Dominguez-López I, Lamuela-Raventós RM. The Chemistry Behind the Folin-Ciocalteu Method for the Estimation of (Poly)phenol Content in Food: Total Phenolic Intake in a Mediterranean Dietary Pattern. *J Agric Food Chem*. 2023;71(46):17543-53. DOI: [10.1021/acs.jafc.3c04022](https://doi.org/10.1021/acs.jafc.3c04022). PMID: 37948650; PMCID: [PMC10682990](https://pubmed.ncbi.nlm.nih.gov/PMC10682990/).
15. Muhtadi M, Haryoto H, Sujono TA, Suhendi A. Antidiabetic and Antihypercholesterolemia Activities of Rambutan (*Nephelium lappaceum* L.) and Durian (*Durio zibethinus* Murr.) Fruit Peel Extracts. *J Appl Pharm Sci*. 2016;6(4):190-4. DOI: [10.7324/JAPS.2016.60427](https://doi.org/10.7324/JAPS.2016.60427).
16. Shraim AM, Ahmed TA, Rahman MM, Hijji YM. Determination of total flavonoid content by aluminum chloride assay: A critical evaluation. *LWT*. 2021;150:111932. DOI: [10.1016/j.lwt.2021.111932](https://doi.org/10.1016/j.lwt.2021.111932).
17. Baliyan S, Mukherjee R, Priyadarshini A, Vibhuti A, Gupta A, Pandey RP, et al. Determination of Antioxidants by DPPH Radical Scavenging Activity and Quantitative Phytochemical Analysis of *Ficus religiosa*. *Molecules*. 2022;27(4):1326. DOI: [10.3390/molecules27041326](https://doi.org/10.3390/molecules27041326). PMID: 35209118; PMCID: [PMC8878429](https://pubmed.ncbi.nlm.nih.gov/PMC8878429/).
18. Mugiyanto E, Cahyanta AN, Putra I, Setyahadi S, Simanjuntak P. Identifying active compounds of soursop ethanolic fraction as α -glucosidase inhibitor. *Pharmaciana*. 2019;9(2):191-200. DOI: [10.12928/pharmaciana.v9i2.10105](https://doi.org/10.12928/pharmaciana.v9i2.10105).

19. Zapata F, López-Fernández A, Ortega-Ojeda F, Quintanilla G, García-Ruiz C, Montalvo G. Introducing ATR-FTIR Spectroscopy through Analysis of Acetaminophen Drugs: Practical Lessons for Interdisciplinary and Progressive Learning for Undergraduate Students. *J Chem Educ.* 2021;98(8):2675-86. DOI: [10.1021/acs.jchemed.0c01231](https://doi.org/10.1021/acs.jchemed.0c01231). PMID: [35281766](https://pubmed.ncbi.nlm.nih.gov/35281766/); PMCID: [PMC8908246](https://pubmed.ncbi.nlm.nih.gov/PMC8908246/).
20. Zhu J, Chen C, Zhang B, Huang Q. The inhibitory effects of flavonoids on α -amylase and α -glucosidase. *Crit Rev Food Sci Nutr.* 2020;60(4):695-708. DOI: [10.1080/10408398.2018.1548428](https://doi.org/10.1080/10408398.2018.1548428). PMID: [30638035](https://pubmed.ncbi.nlm.nih.gov/30638035/).
21. Rauf A, Khan IA, Muhammad N, Al-Awthan YS, Bahattab O, Israr M, et al. Phytochemical composition, in vitro urease, α -glucosidase and phosphodiesterase inhibatroy potency of *Syzygium cumini* (Jamun) fruits. *S Afr J Bot.* 2021;143:418-21. DOI: [10.1016/j.sajb.2021.04.006](https://doi.org/10.1016/j.sajb.2021.04.006).
22. Afendi FM, Okada T, Yamazaki M, Hirai-Morita A, Nakamura Y, Nakamura K, et al. KNApSAcK family databases: integrated metabolite-plant species databases for multifaceted plant research. *Plant Cell Physiol.* 2012;53(2):e1. DOI: [10.1093/pcp/pcr165](https://doi.org/10.1093/pcp/pcr165). PMID: [22123792](https://pubmed.ncbi.nlm.nih.gov/22123792/).
23. Mohanraj K, Karthikeyan BS, Vivek-Ananth RP, Chand RPB, Aparna SR, Mangalapandi P, et al. IMPPAT: A curated database of Indian Medicinal Plants, Phytochemistry And Therapeutics. *Sci Rep.* 2018;8(1):4329. DOI: [10.1038/s41598-018-22631-z](https://doi.org/10.1038/s41598-018-22631-z). PMID: [29531263](https://pubmed.ncbi.nlm.nih.gov/29531263/); PMCID: [PMC5847565](https://pubmed.ncbi.nlm.nih.gov/PMC5847565/).
24. Chen X, Zhai R, Li Y, Yuan X, Liu ZH, Jin M. Understanding the structural characteristics of water-soluble phenolic compounds from four pretreatments of corn stover and their inhibitory effects on enzymatic hydrolysis and fermentation. *Biotechnol Biofuels.* 2020;13:44. DOI: [10.1186/s13068-020-01686-z](https://doi.org/10.1186/s13068-020-01686-z). PMID: [32175010](https://pubmed.ncbi.nlm.nih.gov/32175010/); PMCID: [PMC7065323](https://pubmed.ncbi.nlm.nih.gov/PMC7065323/).
25. Zhong X, Zhang S, Wang H, Yang J, Li L, Zhu J, et al. Ultrasound-alkaline combined extraction improves the release of bound polyphenols from pitahaya (*Hylocereus undatus* Foo-Lon') peel: Composition, antioxidant activities and enzyme inhibitory activity. *Ultrason Sonochem.* 2022;90:106213. DOI: [10.1016/j.ultsonch.2022.106213](https://doi.org/10.1016/j.ultsonch.2022.106213). PMID: [36327918](https://pubmed.ncbi.nlm.nih.gov/36327918/); PMCID: [PMC9636185](https://pubmed.ncbi.nlm.nih.gov/PMC9636185/).
26. Zhang L, Wang Y, Cao Y, Wang F, Li F. Review: Enhancing the Bioavailability and Stability of Anthocyanins for the Prevention and Treatment of Central Nervous System-Related Diseases. *Foods.* 2025;14(14):2420. DOI: [10.3390/foods14142420](https://doi.org/10.3390/foods14142420). PMID: [40724240](https://pubmed.ncbi.nlm.nih.gov/40724240/); PMCID: [PMC12294332](https://pubmed.ncbi.nlm.nih.gov/PMC12294332/).
27. Ilie EI, Popescu L, Luță EA, Biță A, Corbu AR, Mihai DP, et al. Phytochemical Characterization and Antioxidant Activity Evaluation for Some Plant Extracts in Conjunction with Pharmacological Mechanism Prediction: Insights into Potential Therapeutic Applications in Dyslipidemia and Obesity. *Biomedicines.* 2024;12(7):1431. DOI: [10.3390/biomedicines12071431](https://doi.org/10.3390/biomedicines12071431). PMID: [39062004](https://pubmed.ncbi.nlm.nih.gov/39062004/); PMCID: [PMC11274650](https://pubmed.ncbi.nlm.nih.gov/PMC11274650/).
28. Shi L, Zhao W, Yang Z, Subbiah V, Suleria HAR. Extraction and characterization of phenolic compounds and their potential antioxidant activities. *Environ Sci Pollut Res Int.* 2022;29(54):81112-29. DOI: [10.1007/s11356-022-23337-6](https://doi.org/10.1007/s11356-022-23337-6). PMID: [36201076](https://pubmed.ncbi.nlm.nih.gov/36201076/); PMCID: [PMC9606084](https://pubmed.ncbi.nlm.nih.gov/PMC9606084/).
29. Shahidi F, Samarasinghe A. How to assess antioxidant activity? Advances, limitations, and applications of in vitro, in vivo, and ex vivo approaches. *Food Prod Process Nutr.* 2025;7(1):50. DOI: [10.1186/s43014-025-00326-z](https://doi.org/10.1186/s43014-025-00326-z). PMID: [41178997](https://pubmed.ncbi.nlm.nih.gov/41178997/); PMCID: [PMC12572074](https://pubmed.ncbi.nlm.nih.gov/PMC12572074/).
30. Esmaeili AK, Taha RM, Mohajer S, Banisalam B. Antioxidant Activity and Total Phenolic and Flavonoid Content of Various Solvent Extracts from In Vivo and In Vitro Grown *Trifolium pratense* L. (Red Clover). *Biomed Res Int.* 2015;2015:643285. DOI: [10.1155/2015/643285](https://doi.org/10.1155/2015/643285). PMID: [26064936](https://pubmed.ncbi.nlm.nih.gov/26064936/); PMCID: [PMC4438149](https://pubmed.ncbi.nlm.nih.gov/PMC4438149/).
31. Li J, Chen L, Chu X, Ba K, Xie T, Yan W, et al. Synergistic Modulation of π - π^* and n - π^* Transitions by In Situ Phenol-Like Structure Integration for Efficiently Wide-Spectrum Hydrogen Production of Ultrathin Carbon Nitride. *Small.* 2024;20(46):e2405013. DOI: [10.1002/smll.202405013](https://doi.org/10.1002/smll.202405013). PMID: [39109579](https://pubmed.ncbi.nlm.nih.gov/39109579/).

32. Wagner-Wysiecka E, Łukasik N, Biernat JF, Luboch E. Azo group(s) in selected macrocyclic compounds. *J Incl Phenom Macrocycl Chem.* 2018;90(3):189-257. DOI: [10.1007/s10847-017-0779-4](https://doi.org/10.1007/s10847-017-0779-4). Erratum in: *J Incl Phenom Macrocycl Chem.* 2018;90(3):259. DOI: [10.1007/s10847-018-0788-y](https://doi.org/10.1007/s10847-018-0788-y). PMID: 29568230; PMCID: [PMC5845695](https://pubmed.ncbi.nlm.nih.gov/PMC5845695/).
33. Hawryl A, Hawryl M, Chernetskyy M, Winiarski WW, Oniszczyk A. Integrated Chemometric Assessment, Antioxidant Potential, and Phytochemical Fingerprinting of Selected *Stachys* and *Betonica* Plants. *Compounds.* 2026;6(1):14. DOI: [10.3390/compounds6010014](https://doi.org/10.3390/compounds6010014).
34. Chukwuejim S, Kadam D, Aluko RE. Structural, physicochemical, and functional properties of white and blue lupin vicilin and legumin fractions. *Food Chem X.* 2025;31:103078. DOI: [10.1016/j.fochx.2025.103078](https://doi.org/10.1016/j.fochx.2025.103078). PMID: 41080120; PMCID: [PMC12514543](https://pubmed.ncbi.nlm.nih.gov/PMC12514543/).
35. Purwanti N, Roni RAZ, Hakeki AZ, Setiarto RHB. Effects of extraction solvent and isoelectric point on the quality of jack bean (*Canavalia ensiformis*) protein. *Food Sci Biotechnol.* 2024;34(6):1317-25. DOI: [10.1007/s10068-024-01795-7](https://doi.org/10.1007/s10068-024-01795-7). PMID: 40110416; PMCID: [PMC11914563](https://pubmed.ncbi.nlm.nih.gov/PMC11914563/).
36. Han X, Wang P, Zhang J, Lv Y, Zhao Z, Zhang F, et al. α -Glucosidase Inhibition Mechanism and Anti-Hyperglycemic Effects of Flavonoids from *Astragali Radix* and Their Mixture Effects. *Pharmaceuticals.* 2025;18(5):744. DOI: [10.3390/ph18050744](https://doi.org/10.3390/ph18050744). PMID: 40430562; PMCID: [PMC12114633](https://pubmed.ncbi.nlm.nih.gov/PMC12114633/).
37. Assefa ST, Yang EY, Chae SY, Song M, Lee J, Cho MC, et al. Alpha Glucosidase Inhibitory Activities of Plants with Focus on Common Vegetables. *Plants.* 2019;9(1):2. DOI: [10.3390/plants9010002](https://doi.org/10.3390/plants9010002). PMID: 31861279; PMCID: [PMC7020213](https://pubmed.ncbi.nlm.nih.gov/PMC7020213/).
38. Kashtoh H, Baek KH. Recent Updates on Phytoconstituent Alpha-Glucosidase Inhibitors: An Approach towards the Treatment of Type Two Diabetes. *Plants.* 2022;11(20):2722. DOI: [10.3390/plants11202722](https://doi.org/10.3390/plants11202722). PMID: 36297746; PMCID: [PMC9612090](https://pubmed.ncbi.nlm.nih.gov/PMC9612090/).
39. Huong PT, Diep CN, Thanh NV, Tu VA, Hanh TH, Cuong NT, et al. A new cycloartane glucoside from *Rhizophora stylosa*. *Nat Prod Commun.* 2014;9(9):1255-7. DOI: [10.1177/1934578X1400900909](https://doi.org/10.1177/1934578X1400900909). PMID: 25918786.
40. Yang XH, Li HB, Chen H, Li P, Ye BP. [Chemical constituents in the leave of *Rhizophora stylosa* L and their biological activities]. *Yao Xue Xue Bao.* 2008;43(9):974-8. Chinese. PMID: 19048793.
41. Takara K, Kuniyoshi A, Wada K, Kinjyo K, Iwasaki H. Antioxidative flavan-3-ol glycosides from stems of *Rhizophora stylosa*. *Biosci Biotechnol Biochem.* 2008;72(8):2191-4. DOI: [10.1271/bbb.80065](https://doi.org/10.1271/bbb.80065). PMID: 18685199.
42. Li DL, Li XM, Peng ZY, Wang BG. Flavanol derivatives from *Rhizophora stylosa* and their DPPH radical scavenging activity. *Molecules.* 2007;12(5):1163-9. DOI: [10.3390/12051163](https://doi.org/10.3390/12051163). PMID: 17873850; PMCID: [PMC6149341](https://pubmed.ncbi.nlm.nih.gov/PMC6149341/).
43. Fahsi N, Mahdi I, Annaz H, Bitchagno GTM, Mahmoud MF, Sobeh M. Unlocking the therapeutic potential of cinchonans: a comprehensive review. *Phytochem Rev.* 2025;24(1):197-233. DOI: [10.1007/s11101-024-09949-5](https://doi.org/10.1007/s11101-024-09949-5).